Performance tradeoffs among low-complexity detection algorithms for MIMO-LTE receivers

D. Morales-Jiménez*, †, J. F. Paris and J. T. Entrambasaguas

Communication Engineering Department, *University of Málaga*, *Spain*

SUMMARY

The upcoming Third-Generation Partnership Project—Long-Term Evolution (3GPP-LTE) cellular standard will employ spatial multiplexing to significantly increase the data rates. Detection of the spatially multiplexed signals is an essential issue in the design of an LTE receiver. In this paper, we evaluate the performance–complexity tradeoffs for a set of low-complexity multiple input multiple output (MIMO) detection algorithms in a realistic LTE downlink system. Specifically, antenna correlation and channel estimation errors have been considered for a practical MIMO-LTE receiver. An LTE downlink model has been implemented in order to evaluate three types of detectors: linear, unsorted successive interference cancellation (SIC), and ordered SIC. Our simulation results show that the unsorted SIC detectors present a very poor performance–complexity tradeoff. Besides, linear detectors are shown to be the best candidates as the performance improvement for the ordered SIC detectors is not significant in a realistic scenario. Copyright © 2009 John Wiley & Sons, Ltd.

1. INTRODUCTION

Next generation cellular technologies are targeted to provide extremely high data rates over the radio interface. Concretely, the Third-Generation Partnership Project—Long-Term Evolution (3GPP-LTE) technology aims to offer data rates of around 200 Mbps in the downlink and 50 Mbps in the uplink [1]. Multiple antenna techniques, also referred to as multiple input multiple output

*Correspondence to: D. Morales-Jiménez, E.T.S. Ingeniería de Telecomunicación, Campus Universitario de Teatinos, E-29071 Málaga, Spain.
†E-mail: morales@ic.uma.es

(MIMO), are well integrated as a part of the LTE radio access network and will be employed in order to fulfill the LTE initial requirements. In particular, space division multiplexing (SDM) allows increasing data rates by transmitting several data streams simultaneously. The LTE standard defines a *spatial multiplexing* downlink transmission mode, for which up to four data streams may be transmitted by the multiple transmit antennas to the radio interface [2].

The spatially multiplexed streams will interfere with each other due to propagation through the MIMO channel. Thus, multiplexed signals will be overlapped at the receiver side and a MIMO detection stage is needed in order to recover the transmitted data streams.

Several detection algorithms have been proposed for recovering the originally transmitted data streams. Maximum likelihood (ML) detection is optimal but exponentially complex as the number of antennas or the size of transmission alphabet increases. In the descending order of complexity, a number of suboptimal methods range from the successive interference cancellation (SIC) to the simple linear detectors. Non-linear algorithms, such as SIC-based (i.e. decision feedback) [3] or tree-based detectors [4], perform near the optimal, but still at the expense of a high complexity. Reduced-complexity SIC detection algorithms, based on QR matrix decomposition, were proposed in [5, 6]. Linear detection, based on the zero-forcing (ZF) or minimum mean square error (MMSE) criteria, has a lower performance but is considerably less complex than ML.

A performance and complexity analysis of the different detection algorithms is very important as the design and implementation of a practical LTE receiver is vendor specific. A number of works [5–8] address several performance evaluations of different MIMO detection algorithms in the context of Bell Layered Space Time (BLAST) architectures [9]. Most of these works assume ideal conditions, such as perfect knowledge of the channel at the receiver. However, the detection process in a practical receiver is carried out under non-ideal conditions. Specifically, antenna correlation and channel estimation error may significantly degrade the performance of the MIMO detection. Therefore, an in-depth study of this degradation is necessary to evaluate the performance–complexity tradeoffs for the detection algorithms.

In this work, the joint impact of *antenna correlation* and *channel estimation error* on the performance of MIMO detection is addressed. An LTE downlink scenario with two-layer spatial multiplexing and the baseline antenna configuration is considered. Specifically, an LTE model has been implemented on top of WM-SIM platform [10] in order to evaluate the performance of different detectors in a practical MIMO-LTE receiver. Moreover, the performance–complexity tradeoff is shown for a set of pre-selected low-complexity detection algorithms in a realistic MIMO-LTE scenario. Note that, as the MIMO detection is performed at the user equipment, the detector complexity is a crucial issue.

Simulation results show a significant performance improvement when more complex detection algorithms are applied under ideal conditions. However, a gain reduction is observed as the scenario becomes realistic. In other words, the benefit associated with more complex algorithms is significantly reduced when MIMO detection is carried out in a practical scenario, i.e. under non-ideal conditions.

The remainder of this paper is organized as follows. Section 2 provides some useful informations on 3GPP-LTE technology for a better understanding of this work. The LTE downlink system model is presented in Section 3, and the practical channel estimation for LTE downlink is addressed in Section 4. Section 5 provides a brief overview of the different MIMO detection algorithms considered in this work. Simulation results and performance tradeoffs are presented in Section 6. Finally, concluding remarks are gathered in Section 7.

2. SOME ASPECTS ON 3GPP-LTE TECHNOLOGY

The 3GPP-LTE physical layer will offer broadband access to the radio interface at data rates of more than 200 Mbps over the downlink and 50 Mbps over the uplink [1]. These requirements will be fulfilled by employing a combination of new technologies for cellular environments. Concretely, orthogonal frequency division multiplexing (OFDM), and multi-antenna schemes will allow for achieving high data rates and extending coverage. Further details on the 3GPP-LTE technology can be found in [1, 2, 11, 12]. The rest of this section will provide some specific information that can be useful for the understanding of this work.

The LTE downlink transmission is based on OFDM, which is a very efficient modulation technique for wireless systems [13]. Two radio frame structures are supported for frequency division duplex (FDD) and time division duplex (TDD). The FDD radio frame is 10 ms long and consists of 10 subframes of 1 ms duration. One subframe represents the minimum transmission time interval and is composed of two consecutive 0.5 ms time slots, as depicted in Figure 1. Physical resources are organized into a time–frequency grid (see Figure 1), which is defined for each transmit antenna within each time slot. A resource element (RE) corresponds to one OFDM subcarrier and each RE is modulated according to an M-ary quadrature amplitude modulation (M-QAM) scheme. In LTE downlink, supported modulations are: quadrature phase shift keying (QPSK), 16-QAM, and 64-QAM. The number of OFDM subcarriers (from 128 up to 2048) is determined by the transmission bandwidth (from 1.25 to 20 MHz), whereas the number of OFDM symbols per time slot (7 or 6) depends on the cyclic prefix length (normal or extended).

The combination of OFDM with MIMO signal processing, also known as MIMO-OFDM, is employed in order to fulfill the LTE initial requirements in terms of coverage and data rates. Different MIMO-OFDM schemes including transmit diversity and SDM are well integrated as a part of the 3GPP-LTE technology [2]. The *spatial multiplexing* mode will be used for users experiencing a reliable link (i.e. low mobility and good channel conditions). Different MIMO schemes, such as open-loop *transmit diversity* are to be applied for these users with a poor signal-to-noise ratio (SNR) or moving at a high speed.
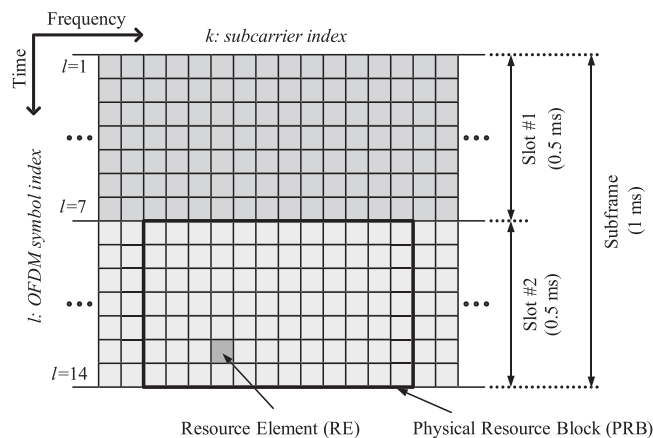

Figure 1. Time–frequency resource grid and subframe structure in LTE.

The baseline antenna configuration in LTE downlink will consist of two antennas at the transmitter and two antennas at the receiver. With the baseline antenna configuration (2×2), a maximum of two layers can be transmitted. Spatial multiplexing is applied together with codebook-based precoding in LTE. However, the set of precoding matrices is reduced to three possible matrices [12] in order to minimize the feedback signalling information and, therefore, the precoding gain is considerably reduced. The predefined codebook also includes the identity matrix, i.e. no precoding is also considered as a special case.

3. LTE DOWNLINK SYSTEM MODEL

The downlink MIMO-OFDM transmission of a simplified LTE system is considered with the baseline antenna configuration. The data for one user are spatially multiplexed into two substreams (also called layers) that are simultaneously transmitted according to the LTE downlink specification [12]. For the scenario under study, no precoding (or equivalently, a fixed precoding matrix equal to the identity) is considered.

3.1. General description

The considered LTE downlink system with two transmit and two receive antennas is depicted in Figure 2. At the transmitter, a single stream of binary input data is transformed into two parallel substreams that are mapped onto M-QAM complex constellation symbols. The complex constellation symbols of each substream are mapped onto the OFDM resource grid, according to the LTE downlink subframe structure (see Section 2). Besides, reference signals (i.e. pilot symbols) are mapped onto the corresponding OFDM subcarriers on each antenna for channel estimation purposes. Therefore, two fully conformed subframes, containing the complex modulation symbols of two substreams, are simultaneously transmitted by the two transmit antennas. Each subframe (i.e. each data substream) is broken into L OFDM sequences of K subcarriers with the ith substream denoted as $x_i(l, k)$, where $l = 1 : L$ and $k = 1 : K$ are, respectively, the time and frequency indexes within a subframe. The OFDM modem at each transmit antenna performs the transformation of the OFDM sequences into the baseband time domain signal.
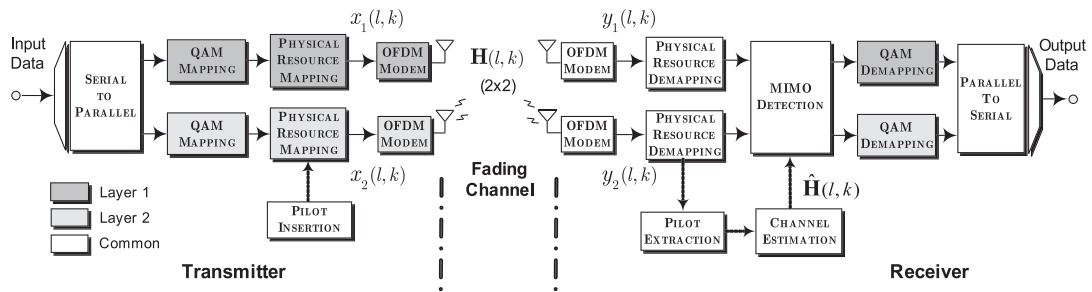

Figure 2. LTE downlink model with 2-layer spatial multiplexing.

After the OFDM modem at each receive antenna, the received sequences can be expressed according to the frequency domain complex baseband model:

$$\mathbf{y}(l,k) = \mathbf{H}(l,k)\mathbf{x}(l,k) + \mathbf{n}(l,k) \tag{1}$$

where $\mathbf{y}(l,k)$ is a bi-dimensional complex vector containing the received symbols for the kth subcarrier of the lth transmitted OFDM sequence. The bi-dimensional complex vector $\mathbf{x}(l,k)$ contains the two corresponding transmitted symbols.

Channel gain is modelled by the (2×2) complex matrix $\mathbf{H}(l,k)$, so that the entries $\mathbf{H} = (h_{ij})$ denote the channel gain between the jth transmit and the ith receive antenna. All channels exhibit frequency-selective slowly time-varying Rayleigh fading and the matrix $\mathbf{H}(l,k)$ is assumed to be spatially correlated. Channel noise is modelled by the bi-dimensional complex vector $\mathbf{n}(l,k)$. The well-known channel noise model is adopted with $\mathbf{n}(l,k)$ additive, Gaussian, and white in space, time, and frequency, i.e. the entries $n_i(l,k)$ are independent and identically distributed (i.i.d.) random variables (RVs) $\sim \mathscr{CN}(0, \sigma_n^2)$. The total average transmit power is normalized to one, and is equally distributed over the two antennas. We define the average SNR $\bar{\gamma}$ in terms of the transmit power constraint and the noise power as $\bar{\gamma} = 1/\sigma_n^2$ [13].

The receiver basically performs the reverse operations of the transmitter. At each receive antenna, the L received OFDM sequences $y_i(l,k)$, with $l = 1 : L$ and $k = 1 : K$, are stored to conform the corresponding received subframe for the ith antenna. Pilot symbols are extracted from each subframe to perform channel estimation (see Section 4). Then, the received complex symbols of both antennas are delivered to the MIMO detection stage, which is in charge of recovering the originally transmitted substreams. After MIMO detection, complex constellation symbols of each substream are de-mapped into binary values.

3.2. MIMO channel model

The standard Rayleigh-faded multi-antenna channel model [14, 15] is considered in this work. To simplify notation, the time and frequency variation of the channel will be omitted hereafter unless otherwise stated. Assuming the well-known Kronecker correlation structure [14], the channel matrix $\mathbf{H}$ can be decomposed as $\mathbf{H} = \mathbf{R}_{rx}^{1/2} \mathbf{G} \mathbf{R}_{tx}^{1/2}$; where the entries of $\mathbf{G}$ are i.i.d. RVs $\sim \mathscr{CN}(0,1)$, and $\mathbf{R}_{tx}, \mathbf{R}_{rx}$ are (2×2) antenna correlation matrices associated with the transmitter and the receiver, respectively. We assume the same antenna correlation factor (ρ) for transmit and for receive antennas. Thus, the correlation matrix is given by

$$\mathbf{R} = \mathbf{R}_{tx} = \mathbf{R}_{rx} = \begin{bmatrix} 1 & \rho \\ \rho^* & 1 \end{bmatrix} \tag{2}$$

where $|\rho| \leqslant 1$. A typical value of ρ in the range $0.3 \leqslant \rho \leqslant 0.7$ will be considered from previous studies on the antenna correlation for a typical suburban environment and uniform linear antenna arrays [16, 17].

4. PRACTICAL LTE CHANNEL ESTIMATION

In LTE downlink, pilot symbols are used to support channel estimation. Pilot symbols are transmitted with a certain arrangement within a subframe (see [2, 12] for details). In the time domain,

pilot symbols are transmitted along the first and third last OFDM symbol intervals of each time slot. Hence, a subframe contains four OFDM symbol intervals (i.e. $l = \{1, 5, 8, 12\}$) with pilot transmission. In the frequency domain, pilots are spread every six subcarriers. With this pilot arrangement, an efficient channel estimation algorithm may apply a 2D time–frequency interpolation to estimate the channel frequency response at all subcarriers within a subframe. Linear interpolation is suitable for the time domain due to the slow variation of the channel. However, frequency selectivity of the channel may be high in a practical scenario with high time dispersion (e.g. with multiple scatterers or in large cells). Therefore, a more accurate interpolation technique is required for the frequency domain. Specifically, two different techniques are *a priori* considered in this work for frequency domain interpolation:

- *Low-pass interpolation* (*LP*) is performed by inserting zeros into the pilot's sequence and then applying a low-pass filter that minimizes the mean square error (MSE) [18].
- The *transform domain processing* (*TD*) is a high-resolution interpolation based on zero-padding, noise filtering, and fast Fourier transform (FFT) [19]. In short, the pilot's sequence is converted into the 'transform domain' by applying an FFT. The resulting sequence is then filtered in order to eliminate noise and zero-padding is performed. Finally, an inverse FFT is applied to convert the sequence back into the frequency domain.

The channel estimation algorithm to obtain each of the entries h_{ij} of the channel matrix **H** is summarized by the following basic steps:

1. Least-square estimation of the channel frequency response at pilot positions for the jth transmit antenna observed at ith receive antenna.
2. Using the samples from step 1, perform interpolation in frequency by using one of the two proposed techniques: LP or TD-based interpolation.
3. Using the results from step 2, perform interpolation in time by applying linear interpolation between the four existing channel estimates within the subframe.

The proposed estimation algorithm for LTE downlink has been evaluated by means of simulations. Figure 3 shows the mean-square error (MSE) of the proposed algorithm, including the two considered candidates for frequency domain interpolation. It is shown that the TD method outperforms the LP interpolator when SNR is below 25 dB. However, the performance of TD is limited in the high SNR regime. Besides, the complexity of the TD method is significantly higher than that of the LP interpolator. Moreover, the 3GPP-LTE specifies the *spatial multiplexing* mode for users under good channel conditions (i.e. high SNR regime), whereas another MIMO schemes will be employed for users with low SNR. Therefore, the LP-based channel estimation has been adopted in this work as the most appropriate for a practical MIMO-LTE receiver.

5. LOW-COMPLEXITY DETECTION ALGORITHMS

The method employed for detection of the different layers plays a significant role in the resulting system performance. The complexity of optimal (i.e. ML) detection is excessively high and makes it unfeasible. Along with the literature, a number of suboptimal solutions range from SIC to simple linear detectors. The objective of this section is to present a set of low complexity detection algorithms that have been pre-selected as feasible candidates for a practical receiver. Specifically, the ZF and MMSE criteria are evaluated for three types of detectors: linear detectors, SIC detectors
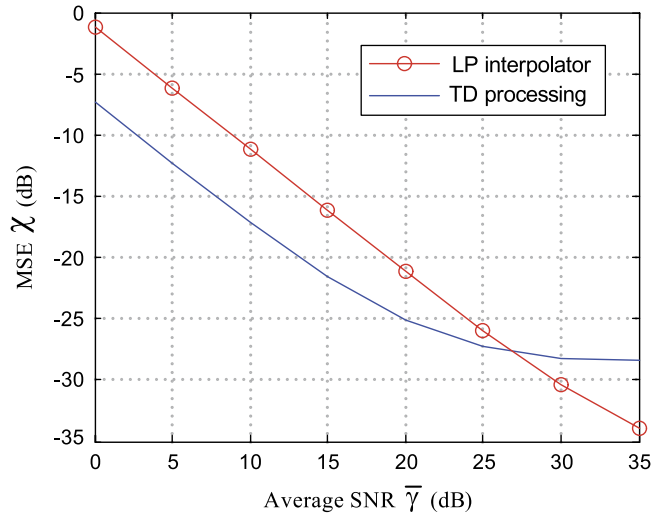
Figure 3. MSE of the proposed channel estimation algorithm with two frequency interpolation techniques. Normalized Doppler shift $fd = 5 \times 10^{-4}$.

with reduced complexity based on QR decomposition (QRD) proposed in [5, 6] (ZF-QRD and MMSE-QRD), and OSIC detectors based on sorted QR decomposition [6] (ZF-SQRD and MMSE-SQRD). Next, we provide a brief overview of these low-complexity detection algorithms.

5.1. Linear detection

In a linear detector, the received symbol vector $\mathbf{y}$ is multiplied by a filter matrix $\mathbf{F}$ as follows:

$$\tilde{\mathbf{x}} = \mathbf{F}\mathbf{y} = \mathbf{F}\mathbf{H}\mathbf{x} + \mathbf{F}\mathbf{n} \tag{3}$$

with the output of the linear detector denoted by the bi-dimensional complex vector $\tilde{\mathbf{x}}$. Then, a parallel decision is performed on all layers. The design of the filter matrix $\mathbf{F}$ depends on the adopted criterion. The well-known ZF and MMSE criteria [20] are considered in this work.

5.2. SIC-based algorithms

When a SIC algorithm is applied, the different layers are not detected in parallel, but one after another. In original BLAST receivers [9], a SIC technique based on the ZF solution was proposed. However, the computational effort is high as a pseudo-inverse calculation is performed for each detection step. Instead, we consider the ZF-QRD (ZF with QR decomposition) algorithm, a very efficient alternative with reduced complexity proposed in [5] that is based on the decomposition of the channel matrix, $\mathbf{H} = \mathbf{Q}\mathbf{R}$; where the (2×2) matrix $\mathbf{Q}$ has orthogonal columns with unit norm and $\mathbf{R}$ is a (2×2) upper triangular matrix. Then, the detected symbol vector $\tilde{\mathbf{x}}$ is obtained by

$$\tilde{\mathbf{x}} = \mathbf{Q}^H \mathbf{y} = \mathbf{R}\mathbf{x} + \mathbf{Q}^H \mathbf{n} \tag{4}$$

and, as $\mathbf{R}$ is upper triangular, the ith detected substream is given by

$$\tilde{x}_i = r_{ii}x_i + \sum_{j=i+1}^{2} r_{ij}x_j + \tilde{n}_i \tag{5}$$

where $\tilde{x}_2$ is free of interference, so that x_2 can be directly estimated. Assuming a correct decision on x_2, the interference can be perfectly cancelled in the next step (i.e. $\tilde{x}_1$).

The QRD algorithm described above can also be extended to the MMSE criterion by considering the extended channel matrix $\underline{\mathbf{H}}$ and the extended receive vector $\underline{\mathbf{y}}$ [6]

$$\underline{\mathbf{H}} = \begin{bmatrix} \mathbf{H} \\ \sigma_n\mathbf{I_2} \end{bmatrix} \quad \text{and} \quad \underline{\mathbf{y}} = \begin{bmatrix} \mathbf{y} \\ \mathbf{0_{2,1}} \end{bmatrix} \tag{6}$$

instead of $\mathbf{H}$ and $\mathbf{y}$. In this case, the algorithm is termed MMSE-QRD.

5.3. Ordered SIC-based algorithms

The detection sequence in the SIC strategy is very important due to the risk of error propagation. The fundamental idea is to perform detection of layers with higher SNR first, which will imply less probability of error propagation.

The order in which the layers are detected can be modified by permuting the elements of $\mathbf{x}$ and the columns of $\mathbf{H}$ prior to QR decomposition [5]. It is clear from (5) that the SNR of the ith layer is determined by $|r_{ii}|^2$. Besides, $|r_{11}|$ is the norm of the first column of $\mathbf{H}$. Therefore, the ordering optimization consists of permuting the column of $\mathbf{H}$ with minimum norm to the first position, so that the layer with minimum SNR is last detected. This algorithm, namely *sorted QR decomposition* (SQRD), was proposed in [5] for the ZF case and extended to the MMSE criterion in [6]. Both ZF-SQRD and MMSE-SQRD algorithms are evaluated in this work.

6. PERFORMANCE TRADEOFF

A performance evaluation of the presented detection algorithms is intended for a practical 3GPP-LTE downlink scenario. Specifically, practical channel estimation and antenna correlation have been introduced in our model in order to evaluate their impact on MIMO detection. The 3GPP-LTE downlink model described in the previous sections has been implemented on top of the WM-SIM simulation platform [10]. WM-SIM is a C++ based and data-flow-oriented platform that allows for implementing and simulating specific complex models.

Simulation parameters are summarized in Table I. We assume the FDD radio frame with normal cyclic prefix, i.e. seven OFDM symbols per slot, and the maximum LTE bandwidth mode (20 MHz). The power delay profile corresponding to a six-taps typical suburban channel [21] is adopted in all the simulations. Channel estimation is performed according to the LP-based algorithm, as discussed in Section 4, and a typical antenna correlation factor above 0.3 [17] is assumed in our practical scenario.

The joint effect of imperfect channel estimation and antenna correlation is illustrated in Figure 4 for all the considered detectors. Bit error rate (BER) is presented as a function of the average SNR for the ZF-based and MMSE-based detectors in Figures 4(a) and (b), respectively. As expected, performance degrades for all the detection algorithms under the presence of antenna correlation

Table I. Simulation parameters.

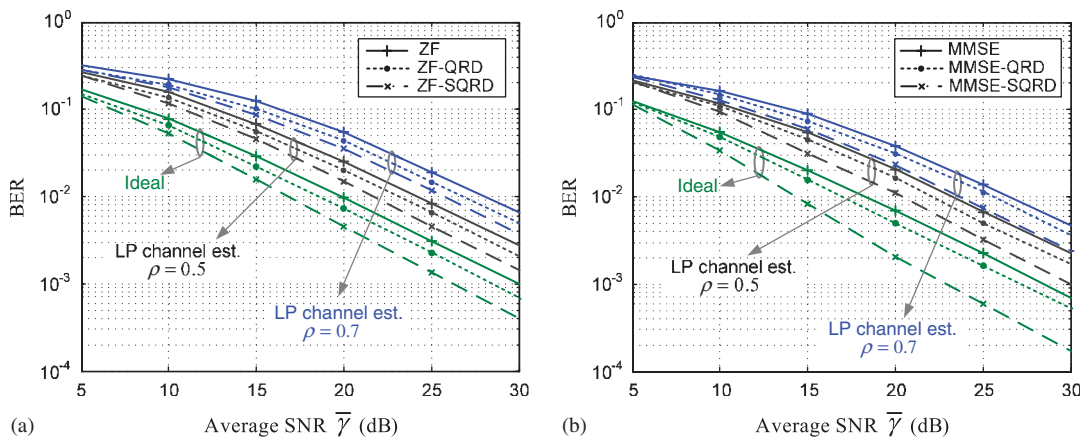| Parameter	Value
Carrier frequency (fc)	1.8 GHz
Sampling frequency (fs)	30.72 MHz
System bandwidth	20 MHz
FFT size	2048
Number of data subcarriers (K)	1200 subcarriers
Cyclic prefix length	144 samples
Subframe duration	1 ms
Simulated time	30 s (30 000 subframes)
User speed	5 km/h (pedestrian)
Pilot-to-data power ratio	1
Modulation scheme	QPSK

Figure 4. Joint impact of imperfect channel estimation and antenna correlation on the performance of linear, SIC, and OSIC detectors: (a) ZF-based algorithms and (b) MMSE-based algorithms.

and channel estimation errors. Besides, the performance improvement associated with SIC (i.e. QRD) and OSIC (i.e. SQRD) detectors is significantly reduced as the antenna correlation increases, specially in the high SNR regime.

An overall performance and complexity evaluation is needed in order to make a conclusion on the tradeoffs among the considered detectors. Figure 5 depicts the performance–complexity tradeoff for the different detection algorithms in a practical MIMO-LTE receiver. Results are presented for two values of antenna correlation, $\rho = 0.3$ and $\rho = 0.5$, together with the ideal case to facilitate a comparison. In order to clarify the comparative analysis, performance is presented as BER in logarithmic units, specifically as $10\log_{10}(BER)$. On the other hand, complexity is expressed in terms of the WM-SIM computation time, which has been normalized to the most complex algorithm (i.e. MMSE-SQRD). Relative computation time for the WM-SIM implementation is reasonably similar to the relative complexity in terms of the number of real valued multiplications, as shown in Table II.
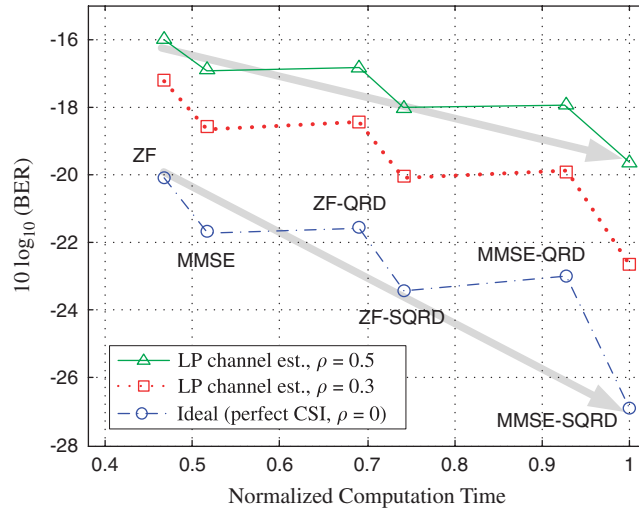
Figure 5. Performance vs computation time for all the considered detection algorithms in a practical MIMO-LTE receiver. Average SNR = 20 dB.

Table II. Complexity in terms of real valued multiplications.*

Detection algorithm	Number of real-valued multiplications	No. mult. ($M = N = 2$)	Relative complexity	Relative computation time
Linear ($M = N$)	$\frac{4}{3}(N^3 + 6N^2 - N)$	40	0.40	0.45
ZF-QRD	$4MN^2 + 4MN + 2N(N+1)$	60	0.60	0.69
ZF-SQRD	$4MN^2 + 6MN + 2N(N+1)$	68	0.68	0.74
MMSE-QRD	$8MN^2 + 4MN + 2N(N+1)$	92	0.92	0.93
MMSE-SQRD	$8MN^2 + 6MN + 2N(N+1)$	100	1.00	1.00

*1 complex multiplication is counted as four real-valued multiplications. Given an $(M \times N)$ channel matrix **H**, the calculations $4MN^2$ and $4MN$ correspond to **QR** decomposition (modified Gram–Schmidt) and multiplication of $\mathbf{Q^H y}$, respectively. Sorting of channel matrix is counted as MN squared norms, which computationally is equivalent to $2MN$ multiplications.

Results from Figure 5 shows that SIC algorithms are considerably more complex than linear detectors for both ZF and MMSE criteria. It is shown that unsorted SIC methods present a very poor performance–complexity tradeoff compared with others (e.g. the MMSE detector outperforms the ZF-QRD, even when the first has less computational cost than the second). Thus, unsorted SIC detectors should be neglected for real-time implementations. On the other hand, a significant performance improvement is achieved when sorting is applied to the detection sequence, i.e. for SQRD algorithms. It is also observed that the computational overhead due to sorting is negligible (about 7% extra computation time from QRD to SQRD). Therefore, when a performance improvement is aimed even at the expense of a higher complexity, a sorted SIC strategy would be the best choice. The overall comparison shows that, once the QRD algorithms are neglected, the performance–complexity tradeoff is approximately defined by a straight line for this particular axis choice (see Figure 5).

In addition, it is observed that an important gain compression takes place as the scenario becomes realistic (see Figure 5). In the ideal case, performance improves by seven points from the least complex (ZF performance ≈ -20) to the most complex algorithm (MMSE-SQRD performance ≈ -27). However, in the case of LP channel estimation and $\rho = 0.5$, the corresponding performance improvement is reduced to four points, which represents more than 40% of gain reduction. That is, the performance improvement associated with more complex detection algorithms is significantly reduced in a practical MIMO-LTE scenario. This can be seen in a graphical way from the slope of the performance–complexity straight line in Figure 5. The slope of this line decreases as the scenario becomes non-ideal (i.e. with practical channel estimation and as the antenna correlation increases). Therefore, it can be concluded that SIC-based algorithms do not provide a significant benefit for real-time implementation in a practical receiver. Instead, the least complex solutions (i.e. linear detectors) could be employed. Specifically, the MMSE linear detector is shown to have an excellent performance–complexity tradeoff in a realistic MIMO-LTE scenario.

7. CONCLUSION

The aim of this work is to evaluate the performance–complexity tradeoffs for a set of detection algorithms in a realistic MIMO-LTE downlink system. Specifically, antenna correlation and channel estimation errors have been considered for a practical receiver with the baseline antenna configuration. An LTE downlink model with two-layer *spatial multiplexing* has been implemented on top of WM-SIM platform in order to evaluate three types of detectors: linear, unsorted SIC (i.e. QRD), and OSIC (i.e. SQRD).

Simulation results show that unsorted SIC detectors present a very poor performance–complexity relation when compared with other detectors (e.g. with a lower complexity, the MMSE linear detector outperforms the ZF-QRD). Therefore, we conclude that QRD algorithms should be neglected for implementation in practical receivers. Besides, OSIC detectors are shown to be a good choice when a performance improvement is aimed even at the expense of a higher complexity. However, the performance gain for SQRD algorithms is significantly reduced when MIMO detection is carried out in a practical scenario (40% reduction with a practical LTE channel estimation and 0.5 antenna correlation factor). Therefore, the benefit associated with SQRD methods is considerably reduced and, thus, linear detectors are the best candidate for a practical LTE receiver.

REFERENCES

1. 3GPP. Requirements for evolved UTRA (E-UTRA) and evolved UTRAN (E-UTRAN). *3GPP Specification TR 25.913* 2006; Release 7, v7.3.0.
2. Gómez G, Morales-Jiménez D, López-Martínez FJ, Sánchez JJ, Entrambasaguas JT. In *3GPP LTE Handbook*, Chapter 3, Furht B, Ahson SA (eds). Auerbach: Boca Raton, FL, U.S.A., 2009. ISBN: 978-1420072105.
3. Foschini GJ, Golden GD, Valenzuela RA, Wolniansky PW. Simplified processing for high spectral efficiency wireless communication employing multi-element arrays. *IEEE Journal on Selected Areas in Communications* 1999; **17**:1841–1852.

4. Jong YLC, Willink TJ. Iterative tree search detection for MIMO wireless systems. *Proceedings of IEEE 56th Vehicular Technology Conference*, Vancouver, Canada, September 2002; 1041–1045.

5. Wübben D, Rinas J, Böhnke R, Kühn V, Kammeyer KD. Efficient algorithm for detecting layered space-time codes. *Proceedings of ITG Conference on Source and Channel Coding*, Berlin, Germany, January 2002; 399–405.

6. Böhnke R, Wübben D, Kühn V, Kammeyer KD. Reduced complexity MMSE detection for BLAST architectures. *Proceedings of the IEEE 46th Global Telecommunications Conference*, San Francisco, U.S.A., vol. 4, December 2003; 2258–2262.

7. Adeane J, Rodrigues MRD, Berenguer I, Wassell IJ. Improved detection methods for MIMO-OFDM-CDM communication systems. *Proceedings of the IEEE 60th Vehicular Technology Conference*, Los Angeles, U.S.A., vol. 3, September 2004; 1604–1608.

8. Li X, Cao X. Low complexity signal detection algorithm for MIMO-OFDM systems. *Electronics Letters* 2005; **41**(2):83–85.

9. Wolniansky PW, Foschini GJ, Golden GD, Valenzuela RA. V-BLAST: an architecture for realizing very high data rates over the rich-scattering wireless channel. *Proceedings of ISSE*, Pisa, Italy, September 1998; 295–300.

10. Sánchez JJ, Morales-Jiménez D, Gómez G, Fernández-Plazaola U, Martos-Naya E, Entrambasaguas JT. WM-SIM: a platform for design and simulation of wireless mobile systems. *Proceedings of the 2nd ACM Workshop on Performance Monitoring and Measurement of Heterogeneous Wireless and Wired Networks*, Chania, Greece, October 2007; 124–127.

11. 3GPP. Long term evolution (LTE) physical layer: general description. *3GPP Specification TS 36.201*, Release 8, v8.1.0, 2007.

12. 3GPP. Physical channels and modulation. *3GPP Specification TS 36.211*, Release 8, v8.1.0, 2007.

13. Goldsmith A. *Wireless Communications*. Cambridge University Press: Cambridge, 2005.

14. Shiu DS, Foschini GJ, Gans MJ, Kahn JM. Fading correlation and its effects on the capacity of multielement antenna systems. *IEEE Transactions on Communications* 2000; **48**(3):502–511.

15. Chizhik D, Farrokhi FR, Ling J, Lozano A. Effect of antenna separation on the capacity of BLAST in correlated channels. *IEEE Communications Letters* 2000; **4**(11):337–339.

16. Lozano A, Tulino AM, Verdu S. Correlation number: a new design criterion in multi-antenna communication. *Proceedings of the IEEE 57th Vehicular Technology Conference* (*VTC'03*), Seoul, Korea, April 2003; 24–28.

17. Pedersen KI, Andersen JB, Kermoal JP, Mogensen PE. A stochastic multiple-input multiple-output radio channel model for evaluations of space-time coding algorithms. *Proceedings of the IEEE 52nd Vehicular Technology Conference* (*VTC'00*), Boston, U.S.A., September 2000; 893–897.

18. Coleri S, Ergen M, Puri A, Bahai A. Channel estimation techniques based on pilot arrangement in OFDM systems. *IEEE Transactions on Broadcasting* 2002; **48**(3):223–229.

19. Zhao Y, Huang A. A novel channel estimation method for OFDM mobile communication systems based on pilot signals and transform domain processing. *Proceedings of the IEEE 47th Vehicular Technology Conference* (*VTC'97*), Phoenix, U.S.A., May 1997; 2089–2093.

20. Verdu S. *Multiuser Detection*. Cambridge University Press: Cambridge, U.K., 1998.

21. 3GPP. Physical layer aspects for evolved universal terrestrial radio access (UTRA). *3GPP Specification TR 25.814*, Release 7, v7.1.0, 2006.

AUTHORS' BIOGRAPHIES

D. Morales-Jiménez received the MSc degree in Telecommunication Engineering from the University of Málaga, Spain, in 2006. Currently, he is with the Communication Engineering Department at the same University, where he works as an associate researcher. His main research interests are related to OFDMA systems, MIMO transmission techniques, MIMO-OFDM detection and interference cancellation.

J. F. Paris received his MSc and PhD degrees in Telecommunication Engineering from the University of Málaga, Spain, in 1996 and 2004, respectively. In 1997 he joined the University of Málaga where he is now an associate professor at the Communication Engineering Department. In 2005, he was with the Stanford University as a visitor associate professor working with Prof. Andrea Goldsmith. His research interests are related to wireless communications, especially wireless access networks, adaptive modulation and diversity systems.

J. T. Entrambasaguas received the MSc and PhD degrees in Telecommunication Engineering from the Polytechnic University of Madrid (UPM), Spain, in 1975 and 1990, respectively. From 1975 to 1978, he was with E.T.S. Ingenieros de Telecomunicación, UPM, Madrid. From 1978 to 1993 he worked at Fujitsu-Spain R&D center, mainly in the development of packet switching systems, data transmission, and hardware/software technology for computer local area networks. In 1993, he joined the University of Málaga where he is now a professor at the Communication Engineering Department. His current research interests include digital signal processing, wireless access networks, power-line communications and methodologies for development and testing of complex communications systems.